Journal of Alloys and Compounds 507 (2010) 521–525

Contents lists available at ScienceDirect

Journal of Alloys and Compounds

journal homepage: www.elsevier.com/locate/jallcom

Thermodynamic modeling of the Pd–Sb system

Wei Han, Mei Li*

Key Laboratory of Superlight Materials and Surface Technology, Ministry of Education, College of Material Science and Chemical Engineering, Harbin Engineering University, Harbin 150001, China

ARTICLE INFO

Article history:
Received 1 June 2010
Received in revised form 30 July 2010
Accepted 30 July 2010
Available online 12 August 2010

Keywords:
Pd–Sb phase diagram
Thermodynamic modeling
CALPHAD technique

ABSTRACT

The Pd–Sb binary system has been thermodynamically assessed by means of CALPHAD approach. The Redlich–Kister polynomial was used to describe the solution phases, liquid (L) and fcc. The non-stoichiometric compound Pd_3Sb and Pd_5Sb_3 were described by a two-sublattice model $(Pd,Sb)_3Sb$ and $(Pd,Sb)_5(Pd,Sb)_3$. The six intermetallic compounds, Pd_8Sb_3, $Pd_{20}Sb_7$, Pd_5Sb_2, Pd_2Sb, PdSb and $PdSb_2$, were treated as stoichiometric phases. The parameters of the Gibbs energy expressions were optimized according to all the available experimental information of both the equilibrium data and the thermodynamic results. A set of self-consistent thermodynamic parameters of the Pd–Sb system has been obtained. The calculations agree well with the respective experimental data.

1. Introduction

Knowledge of phase diagram and thermochemical properties of the Pd–Sb system is very important since these alloying elements are used in several materials of technological importance. For example, the Pd and Sb are the important component elements of Half-Heusler alloys as thermoelectric materials [1,2]. The Pd as contact materials for GaSb and InSb semiconductors, Pd–Sb system has been investigated in contact interface layer [3,4]. And these alloying elements, Pd and Sb, as the main components of most of the currently used catalyst materials has been explored [5]. Hence, a complete thermodynamic description of the Pd–Sb system would prove invaluable to develop alloys for new applications and also provide better understanding of the implications of these alloying elements in existing alloys.

The Pd–Sb system was firstly evaluated by Massalski et al. [6]. In 1991, Durussel and Feschotte [7] redetermined the Pd–Sb phase diagram. On the basis of the results given by Massalski et al. [6] and Durussel and Feschotte [7], Okamoto [8] updated the Pd–Sb phase diagram. But the Pd–Sb system has not been assessed thermodynamically. Therefore, the purpose of this work is to assess the Pd–Sb system by means of the CALPHAD (CALculation of Phase Diagram) technique [9]. The phases of the system are thermodynamically modeled and the parameters of the Gibbs energy expressions are comprehensively optimized.

2. Experimental details

2.1. Experimental phase diagram data

Sander [10] and Grigorjew [11] investigated the Pd–Sb system and determined the invariant temperatures and liquidus temperatures at various compositions by using thermal analysis technique. The phases of Pd_3Sb, PdSb and $PdSb_2$ were found in the Pd–Sb system [10], and a new phase of Pd_5Sb_2 was presented by Grigorjew [11]. Four compounds were found in the region between 25 and 39 at.% Sb below ~1327 K later. Wopersnow and Schubert [12] measured the solubility range for each phase. Massalski et al. [6] drawn the Pd–Sb phase diagram based on experiments [10,11]. The eight compounds, Pd_3Sb, $Pd_{20}Sb_7$, Pd_8Sb_3, $Pd_{31}Sb_{12}$, Pd_5Sb_2, PdSb, and $PdSb_2$, were found in the Pd–Sb system, but the melting reactions of $Pd_{20}Sb_7$, Pd_8Sb_3, $Pd_{31}Sb_{12}$, and Pd_5Sb_2 were unknown. Durussel and Feschotte [7] reinvestigated the Pd–Sb phase diagram by the differential thermal analysis (DTA) and X-ray diffractography. It was found that there are four very narrow and structurally similar phases around Pd_3Sb and these phases formed at very high temperature (between 1479 and 1221 K). And the results showed that thermal stability of these compounds decrease with increasing antimony content. The maximum solid solubility of antimony was reported to be $x_{Sb} = 0.167$ at 1320 K. And the phase of Pd_2Sb existed below 964 K. In the Pd–Sb system [7], the Pd_3Sb, PdSb and $PdSb_2$ melt congruently. Other parts of the Pd–Sb phase diagram were very similar to that shown in reference [6]. The crystal structure of $Pd_{20}Sb_7$, Pd_8Sb_3, Pd_5Sb_2, Pd_3Sb, Pd_5Sb_3, Pd_2Sb, PdSb and $PdSb_2$ were researched by Wopersnow and Schubert [12,13], El-Boragy et al. [14], Bhan and Kudielka [15], Schubert et al. [16], Balz and Schubert [17] and Thomassen [18], respectively. The phase of $Pd_{31}Sb_{12}$

* Corresponding author. Tel.: +86 451 8256 9890; fax: +86 451 8253 3026.
E-mail address: meili206@tom.com (M. Li).

0925-8388/$ – see front matter © 2010 Elsevier B.V. All rights reserved.
doi:10.1016/j.jallcom.2010.07.220

Table 1
The temperature and the composition of the invariant reactions in the Pd–Sb system.

Invariant reaction	Composition of phases (at.% Sb)			Temperature (K)	Reaction type	Ref.
$L \rightarrow Fcc+Pd_3Sb$	21.6	16.7	25.0	1320 ± 2	Eutectic	[7]
	20.2	15.7	25.0	1317	Eutectic	This work
$L \rightarrow Pd_3Sb$	26.4	26.4	–	1479 ± 2	Congruent	[7]
	25.0	25.0	–	1480	Congruent	This work
$Pd_3Sb \rightarrow fcc + Pd_{20}Sb_7$	25.4	16.3	25.9	1213 ± 2	Eutectoid	[7]
	25.0	16.7	25.9	1213	Eutectoid	This work
$Pd_3Sb + Pd_8Sb_3 \rightarrow Pd_{20}Sb_7$	25.5	27.3	25.9	1221 ± 2	Peritectoid	[7]
	25.0	27.3	25.9	1221	Peritectoid	This work
$Pd_3Sb + Pd_5Sb_2 \rightarrow Pd_8Sb_3$	26.7	28.1	27.5	1383 ± 2	Peritectoid	[7]
	25.7	28.5	27.5	1383	Peritectoid	This work
$L + Pd_3Sb \rightarrow Pd_5Sb_2$	30.0	27.0	28.6	1402 ± 2	Peritectic	[7]
	29.8	25.9	28.6	1402	Peritectic	This work
$L + Pd_5Sb_2 \rightarrow Pd_5Sb_3$	36.4	28.6	34.5	1111 ± 2	Peritectic	[7]
	38.7	28.6	35.3	1109	Peritectic	This work
$Pd_5Sb_2 + Pd_5Sb_3 \rightarrow Pd_2Sb$	28.6	34.4	33.3	864	Peritectoid	[7]
	28.6	36.2	33.3	865	Peritectoid	This work
$Pd_5Sb_3 \rightarrow Pd_2Sb + PdSb$	34.5	33.3	50.0	849	Eutectoid	[7]
	36.2	33.3	50.0	848	Eutectoid	This work
$L + Pd_5Sb_3 \rightarrow PdSb$	42.0	38.5	50.0	996	Eutectic	[7]
	42.5	37.6	50.0	1003	Eutectic	this work
$L \rightarrow PdSb$	50.0	50.0		1067 ± 1	Congruent	[7]
	50.0	50.0		1067	Congruent	This work
$L \rightarrow PdSb + Pd_2Sb$	66.6	50.8	66.7	951 ± 2	Eutectic	[8]
	62.4	50.0	66.7	942	Eutectic	This work
$L \rightarrow PdSb_2$	66.7	66.7	–	951 ± 2	Congruent	[8]
	66.7	66.7	–	952	Congruent	This work
$L \rightarrow PdSb + (Sb)$	88.0	66.7	100.0	860 ± 1	Eutectic	[7]
	85.3	66.7	100.0	865	Eutectic	This work

is not included because it was the only phase with an unknown crystal structure.

The temperature and the compositions of the invariant reaction in the Pd–Sb system were listed in Table 1 and crystal structure data of the phases [8] in the Pd–Sb system were listed in Table 2.

2.2. Thermodynamic data

The heat of formation at 298 K was determined by calorimetry for the fcc phase palladium-rich alloys and the intermediate phases PdSb and $PdSb_2$. The experimental results were reported to be −47.42 and −38.90 kJ/mol of atoms for PdSb and $PdSb_2$, respectively [19].

3. Thermodynamic models

3.1. Pure elements

The stable forms of the pure elements at 298.15 K were chosen as the reference states of the system. For the thermodynamic functions of the pure elements in their stable and metastable states, the phase stability equations compiled by Dinsdale [20] were used in the present optimization. The equations are of the SGTE (Scientific Group Thermodata Europe) format:

$$ {}^0G_i^{\phi}(T) = G_i^{\phi}(T) - H_i^{SER}(298.15\,\mathrm{K}) = a + bT + cT\ln T + dT^2 + eT^3 + fT^{-1} + gT^7 + hT^{-9} \quad (1) $$

where H_i^{SER} (298.15 K) is the molar enthalpy of the element i at 298.15 K in its standard element reference (SER) state, fcc for Pd and rhombohedral for Sb. $G_i^{\phi}(T)$ and ${}^0G_i^{\phi}(T)$ are the absolute and the relative Gibbs energy of the element i in the ϕ state. The Gibbs energy of the element i (i = Pd and Sb), ${}^0G_i^{\phi}(T)$, in its SER state is denoted by $GHSER_i$, i.e.

$$ GHSER_{Pd} = {}^0G_{Pd}^{fcc}(T) = G_{Pd}^{fcc}(T) - H_{Pd}^{SER}(298.15\,\mathrm{K}) \quad (2) $$

$$ GHSER_{Sb} = {}^0G_{Sb}^{rhom}(T) = G_{Sb}^{rhom}(T) - H_{Sb}^{SER}(298.15K) \quad (3) $$

3.2. Solution phases

In the Pd–Sb system, the solution phases, liquid and fcc, were described by the substitutional solution model. The Gibbs energy function of the solution phase ϕ for 1 mole of atoms is described by

Table 2
Crystal structure data of the phases in the Pd–Sb system[a].

Phase	Composition (at.% Sb)	Pearson symbol	Strukturbericht designation	Space group	Prototype
(Pd)	0–16.7	cF4	A1	$Fm\bar{3}m$	Cu
Pd_3Sb	25.0–27.0	cF16	B32	$Fd\bar{3}m$	NaTl
$Pd_{20}Sb_7$	25.9	hR27	–	$R\bar{3}$	–
Pd_8Sb_3	27.5	hR44	–	$R\bar{3}c$	–
Pd_5Sb_2	27.7–28.3	hP84	–	$p6_3/mmc$	–
Pd_2Sb	33.3	oC24	–	$Cmc2_1$	–
Pd_5Sb_3	34.3–38.5	hP4	$B8_1$	$p6_3/mmc$	NiAs
PdSb	50.0–50.8	hP4	$B8_1$	$p6_3/mmc$	NiAs
$PdSb_2$	66.7	cP12	FeS_2(pyrite)	Pa3	FeS_2(pyrite)
(Sb)	100	hR2	αAs	$R\bar{3}m$	αAs

[a] Crystal structures are taken from Okamoto [8].

the following expression:

$$G_m^{\phi} = x_{Pd}{}^0G_{Pd}^{\phi} + x_{Sb}{}^0G_{Sb}^{\phi} + RT(x_{Pd}\ln x_{Pd} + x_{Sb}\ln x_{Sb}) + {}^EG_m^{\phi} \quad (4)$$

where ${}^0G_i^{\phi}$ is the molar Gibbs energy of the element i (i = Pd and Sb) with the structure of ϕ. ${}^EG_m^{\phi}$ is the excess Gibbs energy which is expressed in Redlich–Kister polynomial:

$${}^EG_m^{\phi} = x_{Pd}x_{Sb}\sum_i {}^iL^{\phi}(x_{Pd} - x_{Sb})^i \quad (5)$$

The parameter ${}^iL^{\phi}$ (i = 0,1,2,...) is the ith interaction parameter between the elements Pd and Sb and to be evaluated in the present work. Its general form is as the following:

$${}^iL^{\phi} = a_i + b_iT + c_iT\ln T + d_iT^2 + e_iT^3 + f_iT^{-1} + g_iT^7 + h_iT^{-9} \quad (6)$$

where a_i, b_i, c_i, d_i, e_i, f_i, g_i and h_i are the coefficients to be optimized. In most cases, only the first one or two terms of the above equation are used.

3.3. Stoichiometric compounds

In the present optimization, Pd_5Sb_3, $Pd_{20}Sb_7$, Pd_5Sb_2, Pd_2Sb, PdSb and $PdSb_2$ phases, with narrow or nil solubility ranges were treated as the stoichiometric compounds. The Gibbs energy per mole of formula unit Pd_mSb_n is expressed as follows:

$$\begin{aligned}{}^0G_m^{Pd_mSb_n} &= G_m^{Pd_mSb_n} - mH_{Pd}^{SER} - nH_{Sb}^{SER} \\ &= m{}^0G_{Pd}^{fcc} + n{}^0G_{Sb}^{rhom} + \Delta G_f^{Pd_mSb_n}\end{aligned} \quad (7)$$

where $\Delta G_f^{Pd_mSb_n}$ is the Gibbs energy of formation for per mole of formula unit Pd_mSb_n. $\Delta G_f^{Pd_mSb_n}$ can be given by the following expression:

$$\Delta G_f^{Pd_mSb_n} = a + bT \quad (8)$$

where a and b are the parameters to be evaluated in the present work.

3.4. Intermediate phases with homogeneity range

3.4.1. The Pd_3Sb phase

The intermediate phase Pd_3Sb has a wide composition range to the Sb-rich side of the strict stoichiometric Pd_3Sb. The two sublattice model [21,22], (Pd%,Sb)$_3$Sb was used in this case. The symbol % denotes the major component in the corresponding sublattice. The Gibbs energy function of the Pd_3Sb phase is as the following:

$$\begin{aligned}G_m^{Pd_3Sb} - H_{Pd_3Sb}^{SER} &= y_{Pd}^{I}{}^0G_m^{Pd_3Sb} + y_{Sb}^{I}{}^0G_m^{Sb_3Sb} + 3RT(y_{Pd}^{I}\ln y_{Pd}^{I} \\ &\quad + y_{Sb}^{I}\ln y_{Sb}^{I1}) + y_{Pd}^{I}y_{Sb}^{I}L_{Pd,Sb:Sb}^{(Pd\%,Sb)_3Sb}\end{aligned} \quad (9)$$

$$L_{Pd,Sb:Sb}^{(Pd\%,Sb)_3Sb} = \sum_{n=0}(a_n + b_nT)(y_{Pd}^{I} - y_{Sb}^{I})^n \quad (10)$$

where $H_{Pd_3Sb}^{SER}$ is the abbreviation of $3y_{Pd}^{I}H_{Pd}^{SER} + (1 + 3y_{Sb}^{I})H_{Sb}^{SER}$. y_i^{I} is the site fractions of the component i (i = Pd and Sb) in the first sublattice. ${}^0G_m^{Pd_3Sb}$ and ${}^0G_m^{Sb_3Sb}$ are the Gibbs energies of the stoichiometric and hypothetic compounds Pd_3Sb and Sb_3Sb respectively, as were modeled by Eqs. (7) and (8). $L_{Pd,Sb:Pd}^{(Pd,Sb)_3Sb}$ is the interaction parameter between the elements Pd and Sb in the first sublattice as was modeled by Eq. (10).

3.4.2. The Pd_5Sb_3 phase

The intermediate phase Pd_5Sb_3, having a homogeneity range, was treated as (Pd%,Sb)$_5$(Pd,Sb%)$_3$ by a two-sublattice model [21,22]. The Gibbs energy per mole of the formula unit (Pd%,Sb)$_5$(Pd,Sb%)$_3$ is given by the following expression:

$$\begin{aligned}G_m^{(Pd\%,Sb)_5(Pd,Sb\%)_3} &- H_{(Pd\%,Sb)_5(Pd,Sb\%)_3}^{SER} \\ &= y_{Pd}^{I}y_{Pd}^{II}{}^0G_m^{Pd_5Pd_3} + y_{Pd}^{I}y_{Sb}^{II}{}^0G_m^{Pd_5Sb_3} + y_{Sb}^{I}y_{Pd}^{II}{}^0G_m^{Sb_5Pd_3} \\ &\quad + y_{Sb}^{I}y_{Sb}^{II}{}^0G_m^{Sb_5Sb_3} + 5RT(y_{Pd}^{I}\ln y_{Pd}^{I} + y_{Sb}^{I}\ln y_{Sb}^{I}) + 3RT(y_{Pd}^{II}\ln y_{Pd}^{II} \\ &\quad + y_{Sb}^{II}\ln y_{Sb}^{II}) + {}^EG_m^{(Pd\%,Sb)_5(Pd,Sb\%)_3}\end{aligned} \quad (11)$$

where $H_{(Pd\%,Sb)_5(Pd,Sb\%)_3}^{SER}$ is the abbreviation of $(5y_{Pd}^{I} + 3y_{Pd}^{II})H_{Pd}^{SER} + (5y_{Sb}^{I} + 3y_{Sb}^{II})H_{Sb}^{SER}$. y_i^{I} and y_i^{II} are the site fractions of the component i (i = Pd and Sb) in the first and the second sublattices, respectively. ${}^0G_m^{Pd_5Pd_3}$, ${}^0G_m^{Pd_5Sb_3}$, ${}^0G_m^{Sb_5Pd_3}$ and ${}^0G_m^{Sb_5Sb_3}$ represent the Gibbs energies of the hypothetic and stoichiometric compounds Pd_5Pd_3, Pd_5Sb_3, Sb_5Pd_3 and Sb_5Sb_3, formed when each of the sublattices is occupied by only one component Pd or Sb (y_{Pd} = 1 or y_{Sb} = 1), and they were modeled by Eqs. (7) and (8). ${}^EG_m^{(Pd\%,Sb)_5(Pd,Sb\%)_3}$ is the excess Gibbs energy expressed by the following expression:

$$\begin{aligned}&{}^EG_m^{(Pd\%,Sb)_5(Pd,Sb\%)_3} \\ &= y_{Pd}^{I}y_{Sb}^{I}(y_{Pd}^{II}L_{Pd,Sb:Pd}^{(Pd\%,Sb)_5(Pd,Sb\%)_3} + y_{Sb}^{II}L_{Sb:Pd,Sb}^{(Pd\%,Sb)_5(Pd,Sb\%)_3}) \\ &\quad + y_{Pd}^{II}y_{Sb}^{II}(y_{Pd}^{I}L_{Pd:Pd,Sb}^{(Pd\%,Sb)_5(Pd,Sb\%)_3} + y_{Sb}^{I}L_{Sb:Pd,Sb}^{(Pd\%,Sb)_5(Pd,Sb\%)_3})\end{aligned} \quad (12)$$

$$L_{Pd,Sb:k}^{(Pd\%,Sb)_5(Pd,Sb\%)_3} = \sum_{n=0}(a_n + b_nT)(y_{Pd}^{I} - y_{Sb}^{I})^n \quad (13)$$

$$L_{k:Pd,Sb}^{(Pd\%,Sb)_5(Pd,Sb\%)_3} = \sum_{n=0}(a_n + b_nT)(y_{Pd}^{II} - y_{Sb}^{II})^n \quad (14)$$

where $L_{k:Pd,Sb}^{(Pd\%,Sb)_5(Pd,Sb\%)_3}$ and $L_{Pd,Sb:k}^{(Pd\%,Sb)_5(Pd,Sb\%)_3}$ represent the interaction parameters between the elements Pd and Sb in the related sublattice while the other sublattice is occupied only by the element k (k = Pd and Sb).

4. Assessment procedure

The thermodynamic optimization of the model parameters of the Gibbs energy expressions is an application of the CALPHAD technique with the help of the PARROT module of the Thermo-Calc software developed by Jansson [23] and Sundman et al. [24]. Its procedure consists of the choice of thermodynamic models for the Gibbs energy of the individual phases as previously described, the analysis of all the related experimental data available, and the computer-aided nonlinear regression for minimizing the square sum of the errors between the experimental data and the computed values.

The experimental data from Sander [10], Grigorjew [11], and Durussel and Feschotte [7] were used in the optimization. The data from [4,11] were offered relatively large weight factors since they had constructed a reasonable phase diagram over almost the entire composition range. In this study, the thermodynamic parameters for the intermetallic compounds were optimized at the first stage based on standard enthalpies of formation for the Pd–Sb intermetallic compounds [19] and the phase boundary information [10,11].

The ${}^0G_m^{Pd_5Pd_3}$ and ${}^0G_m^{Sb_5Sb_3}$ with Pd_5Sb_3 structure in Eq. (9) are the hypothetical forms of the corresponding pure elements, and the parameter a of their Gibbs energy expression as shown in Eq. (8) was ensured to be a sufficiently positive value relative to their SER state. In order to reduce the number of optimizing variables, it was assumed that $L_{Pd,Sb:Pd}^{(Pd\%,Sb)_5(Pd,Sb\%)_3} = L_{Pd,Sb:Sb}^{(Pd\%,Sb)_5(Pd,Sb\%)_3}$, $L_{Pd:Pd,Sb}^{(Pd\%,Sb)_5(Pd,Sb\%)_3} = L_{Sb:Pd,Sb}^{(Pd\%,Sb)_5(Pd,Sb\%)_3}$.

Table 3
The thermodynamic parameters of the Pd–Sb system[a].

Phase	Parameters
Liquid	${}^0L^{Liquid} = -186,656.4 + 42.548 \times T$
	${}^1L^{Liquid} = -95,651.8 + 32.036 \times T$
fcc	${}^0L^{Fcc} = -176,510.8 + 46.406 \times T$
	${}^1L^{Fcc} = -902,35.1 + 22.051 \times T$
Pd_3Sb	${}^0G_m^{Pd_3Sb} = 3{}^0G_{Pd}^{fcc} + {}^0G_{Sb}^{rhom} - 134,392.8 - 5.305 \times T$
	${}^0G_m^{Sb_3Sb} = 4{}^0G_{Sb}^{rhom} + 20,000$
	${}^0L_{Pd,Sb:Sb}^{Pd_3Sb} = -215,273.1 + 5.049 \times T$
$Pd_{20}Sb_7$	${}^0G_m^{Pd_{20}Sb_7} = 20{}^0G_{Pd}^{fcc} + 7{}^0G_{Sb}^{rhom} - 1064,845.5 + 72.808 \times T$
Pd_8Sb_3	${}^0G_m^{Pd_8Sb_3} = 8{}^0G_{Pd}^{fcc} + 3{}^0G_{Sb}^{rhom} - 447,831.9 + 28.997 \times T$
Pd_5Sb_2	${}^0G_m^{Pd_5Sb_2} = 5{}^0G_{Pd}^{fcc} + 2{}^0G_{Sb}^{rhom} - 290,622.9 + 18.047 \times T$
Pd_2Sb	${}^0G_m^{Pd_2Sb} = 2{}^0G_{Pd}^{fcc} + {}^0G_{Sb}^{rhom} - 131,878.8 + 13.981 \times T$
Pd_5Sb_3	${}^0G_m^{Pd_5Sb_3} = 5{}^0G_{Pd}^{fcc} + 3{}^0G_{Sb}^{rhom} - 324,579.4 + 2.999 \times T$
	${}^0G_m^{Pd_5Pd_3} = 8{}^0G_{Pd}^{fcc} + 40000$
	${}^0G_m^{Sb_5Sb_3} = 8{}^0G_{Sb}^{rhom} + 40000$
	${}^0G_m^{Sb_5Pd_3} = 5{}^0G_{Sb}^{rhom} + 3{}^0G_{Pd}^{fcc} - 40,036.0 + 10.001 \times T$
	$L_{Pd,Sb:Pd}^{Pd_5Sb_3} = -344,444.1 + 145.001 \times T$
	$L_{Pd,Sb:Sb}^{Pd_5Sb_3} = -344,444.1 + 145.001 \times T$
	$L_{Pd:Pd,Sb}^{Pd_5Sb_3} = -397,728.0 + 130.183 \times T$
	$L_{Sb:Pd,Sb}^{Pd_5Sb_3} = -397,728.0 + 130.183 \times T$
PdSb	${}^0G_m^{PdSb} = {}^0G_{Pd}^{fcc} + {}^0G_{Sb}^{rhom} - 95,313.7 + 13.768 \times T$
$PdSb_2$	${}^0G_m^{PdSb_2} = {}^0G_{Pd}^{fcc} + 2{}^0G_{Sb}^{rhom} - 112,527.2 + 19.884 \times T$

[a] In J/(mole of formula units); temperature (T) in K.

The optimization of Pd_3Sb and Pd_5Sb_3 were carried out in two steps. In the first, Pd_3Sb and Pd_5Sb_3 were assumed to be a stoichiometric compound. And in the second, they were treated using two-sublattice model. The parameters obtained from the first treatment were used as starting values for the second.

In the beginning of the assessment, each item of the selected information was given a certain weight factor by judgment. During the period of optimization, the weight factors were adjusted by trial and error. The final data set was obtained when the squared sum of the errors between the experimental data and the calculated results was reduced to a certain level.

5. Results and discussion

The thermodynamic description and the optimized parameters of the Pd–Sb system are listed in Table 3. The calculated Pd–Sb phase diagram is compared with the experimental data [10,11] in Fig. 1 and is nearly identical to the one represented by Sander [10] and Grigorjew [11]. With respect to the $PdSb_2$ phase, a peritectic transformation was suggested in previous works [10,11]. Moreover, the phase diagram reported by Durussel and Feschotte [7] is not completely clear on this point. Because the incompatible asymmetry of the liquidus on the left and right sides of the compound PdSb, the $PdSb_2$ phase should melt congruently. Okamoto [8] updated the Pd–Sb system, and pointed the $PdSb_2$ phase melts congruently.

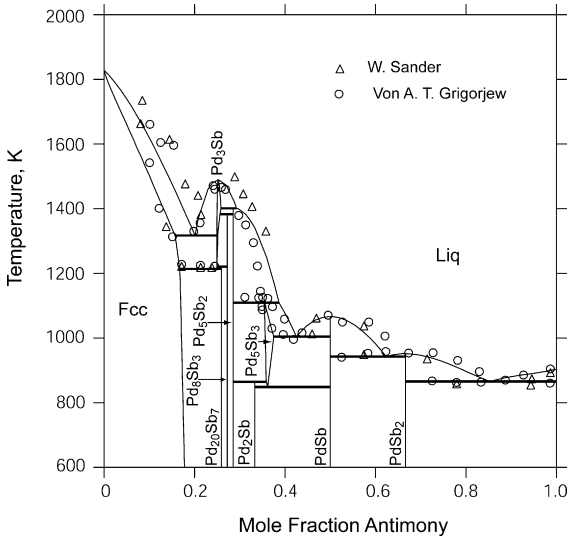

Fig. 1. The calculated Pd–Sb phase diagram compared with the experimental data [10,11].

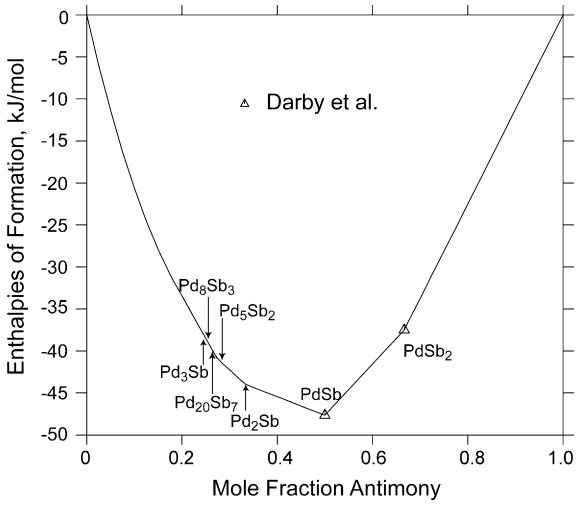

Fig. 2. The calculated formation enthalpies of the Pd–Sb system with experimental measurements at 298 K [19].

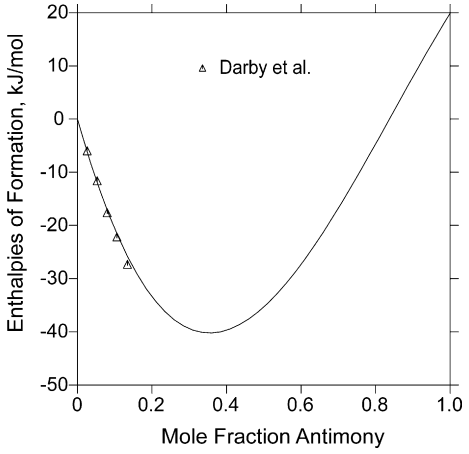

Fig. 3. The calculated standard enthalpies of formation of the fcc phase palladium-rich alloys at 298 K with experimental data [19].

All invariant equilibria in the system given by Durussel and Feschotte [7] are reproduced, which are listed in Table 1. The compositions and temperatures of invariant reactions fit well with the experiments [7]. Figs. 2 and 3 show the calculated the heat of formation at 298 K for the fcc phase palladium-rich alloys and the intermediate phases PdSb and $PdSb_2$ in the Pd–Sb system with the experimental data determined by Darby et al. [19].

Within the experimental uncertainties, most of the experimental data are well reproduced by the present calculation.

6. Conclusions

All of the experimental phase equilibria and thermodynamic data of the Pd–Sb system from the available literature have

been critically evaluated. Within the regime of CALPHAD technique, the Redlich-Kister polynomial, the sublattice-compound energy model and the temperature dependant expression were adopted to describe the solution phases, the non-stoichiometric phases and the stoichiometric compounds, respectively. After the optimization of the Gibbs energy functions, a set of consistent thermodynamic parameters for the Pd–Sb binary system is obtained. The calculated phase equilibria and thermodynamic properties, including the phase diagrams and the standard enthalpies of formation for the Pd–Sb intermetallic compounds, all agree well with the experimental data. With the thermodynamic description available, one can now make various calculations of practical interest. Detailed experiments are necessary to check these inconsistencies.

Acknowledgements

The authors would like to express their appreciation to the Royal Institute of Technology Sweden for supplying the Thermo-Calc software.

References

[1] J. Navrátil, F. Laufek, T. Plechácek, J. Plášil, J. Alloys Compd. 493 (2010) 50.
[2] T. Harmening, H. Eckert, R. Pöttgen, Solid State Sci. 11 (2009) 900.
[3] J.A. Robinson, S.E. Mohney, J. Electron Mater. 35 (2006) 48.
[4] H. Ipser, K.W. Richter, J. Electron Mater. 32 (2003) 1136.
[5] G. Suresh, J. Radnik, V.N. Kalevaru, M.-M. Pohl, M. Schneider, B. Lücke, A. Martin, A. Brückner, Phys. Chem. Chem. Phys. 12 (2010) 4833.
[6] T.B. Massalski, H. Okamoto, P.R. Subramanian, L. Kacprzak, Binary Alloy Phase Diagrams, 2nd ed., ASM International, Materials Park, OH, 1990.
[7] P. Durussel, P. Feschotte, J. Alloys Compd. 176 (1991) 173.
[8] H. Okamoto, J. Phase Equilib. 13 (1992) 578.
[9] L. Kaufman, H. Berhstein, Computer Calculation of Phase Diagrams, Academic Press, New York, NY, 1970.
[10] W. Sander, Z. Anorg. Allg. Chem. 75 (1912) 97.
[11] A.T. Von, Grigorjew, Z. Anorg. Allg. Chem. 209 (1932) 308.
[12] Wopersnow, Schubert, J. Less-Common Met. 51 (1977) 35.
[13] Wopersnow, Schubert, J. Less-Common Met. 48 (1976) 79.
[14] M. El-Boragy, S. Bhan, K. Schubert, J. Less-Common Met. 22 (1970) 445.
[15] S. Bhan, H. Kudielka, Z. Metallkd. 69 (1978) 333.
[16] K. Schubert, K. Anderko, M. Kulge, H. Beeskow, et al., Naturwissenschaften 40 (1953) 269.
[17] U. Balz, K. Schubert, J. Less-Common Met. 19 (1969) 300.
[18] L. Thomassen, Z. Phys. Chem. 135 (1928) 383.
[19] J.B. Darby Jr., K.M. Myles, J.N. Pratt, Acta Met. 19 (1971) 7.
[20] A.T. Dinsdale, Calphad 15 (1991) 317.
[21] B. Sundman, J. Agren, J. Phys. Chem. Solids 42 (1981) 297.
[22] M. Hillert, L.I. Staffansson, Acta Chem. Scand 24 (1970) 3618.
[23] B. Jansson, Ph.D. thesis, Royal Institute of Technology, Stockholm, Sweden, 1984.
[24] B. Sundman, B. Jansson, J.-O. Andersson, Calphad 2 (1985) 153.